REVISTA INTERDISCIPLINAR DE PESQUISA EM ENGENHARIA

CILAMCE 2016
XXXVII IBERIAN LATIN AMERICAN CONGRESS ON COMPUTATIONAL METHODS IN ENGINEERING
BRASÍLIA - DF - BRAZIL

SIMULATION OF NATURALLY FRACTURED RESERVOIRS USING SINGLE-POROSITY EQUIVALENT MODELS

Robison Quintana Saalfeld

saalfeld@dep.fem.unicamp.br

João Carlos Von Hohendorff Filho

joao@dep.fem.unicamp.br

Denis José Schiozer

denis@cepetro.unicamp.br

Universidade Estadual de Campinas

Cidade Universitária Zeferino Vaz – Barão Geraldo, Campinas, 13083-970, São Paulo, Brasil.

Abstract. *Brazilian Pre-Salt reservoirs are composed of very heterogeneous carbonate rocks with high permeability layers. Double-porosity models are usually applied for the simulation of such systems. In double-porosity models, the rock matrix and the fractures are idealized as two different porous media, modeled as two spatially coincident grids related by a transfer function. However, double-porosity models require solving more equations and, consequently, demand more computational time to simulate than conventional single-porosity reservoir models. An alternative to simulate heterogeneous reservoirs more efficiently is to use pseudo properties that account for both media in a single-continuum equivalent model. This work presents a methodology to obtain similar results of double-porosity models through the use of conventional single-porosity reservoir models with pseudo properties. The methodology is applied to 280 homogeneous isotropic models composed by different combinations of properties, classified accordingly to characteristic naturally fractured reservoir parameters. For 97% of the tested models, the methodology was able to obtain single-porosity equivalent models that resemble the behavior of double-porosity with error below 10%. For the availed cases, the use of single-porosity models implies a reduction of up to 33 times in computational time, which may allow more studies in order to obtain better reservoir management.*

Keywords: *Naturally fractured, Pseudo relative permeability, Single-porosity, Double-porosity, Reservoir simulation*

1 INTRODUCTION

Naturally fractured reservoirs are usually simulated through double-porosity models. The first approach of dual-porosity is presented by Barenblatt et al. (1960). In their work, the continuum hypothesis is assumed for the fractures network, so that it acts as an equivalent porous medium. The two porous media, the fracture network and the porous matrix, are related by a source-sink term called transfer function, which establishes how the matrix blocks feed the fractures.

The work by Warren & Root (1963) is the first to provide a formulation for the transfer function and an approximate solution for the dual-porosity model for analysis of transient well testing. In their model, the transfer between matrix and fractures is assumed to occur always on pseudosteady state, and the rate of transfer depends on both permeabilities of the system, the pressure gradient between fractures and matrix at a given point, and a geometrical factor that accounts for the dimensions of the matrix block. Warren & Root considered that since fracture permeability is usually far greater than that of the porous matrix, the flow could be considered to take place only between fracture-fracture and matrix-fracture, ignoring flow between two matrix blocks.

Warren & Root defined two dimensionless parameters to characterize the response of the double-porosity system: the storativity ratio ω, defined as in Eq. (1)

$$\omega = \frac{c_f \varnothing_f}{c_f \varnothing_f + c_m \varnothing_m} \tag{1}$$

and the inter-porosity transfer parameter λ, defined in Eq. (2)

$$\lambda = 60 \frac{k_m r_w^2}{k_f L^2} \tag{2}$$

where c is the total compressibility of the medium, $\varnothing$ is the porosity of the medium in respect to total volume of the system, k is the permeability, r_w is the production well radius and L is the mean space between fracture planes. The subscripts m and f will therefore denote porous matrix and fracture media, respectively. Fracture medium properties are uspcaled averages of the actual fractures present in a grid block, so k_f is the equivalent permeability provided by the fractures to fluid transmissibility in the block and $\varnothing_f$ is the ratio between fracture volume and grid block volume.

Kazemi et al. (1976) extended the equations of Warren & Root (1963) for two-phase flow in fractured reservoirs, but their transfer function does not account for gravitational effects. Thomas et al. (1983) presents a three-phase model, which accounts for gravity effects by the use of pseudo relative permeability and capillary pressure curves. The formulation for a fluid phase α moving in a double porosity system is presented in Eqs. (3) to (5):

$$\nabla \cdot \left[\frac{k_f k_{\alpha r,f}}{\mu_{\alpha f} B_{\alpha f}} \nabla \Phi_{\alpha f} \right] - \tau_\alpha + q = \frac{\partial}{\partial t} \left(\frac{\varnothing_f S_{\alpha f}}{B_{\alpha f}} \right) \tag{3}$$

$$\tau_{\alpha} = \frac{\partial}{\partial t}\left(\frac{\emptyset_m S_{\alpha m}}{B_{\alpha m}}\right) \tag{4}$$

$$\tau_{\alpha} = -\frac{k_{r\alpha m}}{B_{\alpha m}\mu_{\alpha m}}\sigma k_m\left(\Phi_{\alpha m} - \Phi_{\alpha f}\right) \tag{5}$$

where μ stands for the viscosity, B is the formation volume factor, Φ is the potential, S is the saturation, τ is the transfer function, q is the well rate function (positive for injection, negative for production or zero for blocks with no well). σ is the *shape factor*, which is a factor that accounts for geometry dependence on the fluid transfer from matrix blocks to fractures.

1.1 Pseudo properties approach

Another approach for the simulation of naturally fractured reservoirs is the application of pseudo properties that account for the effect of fractures on a single-porosity system. The basic assumption under this technique is that, under specific conditions, the system described in Eqs (3) to (5) has a response similar to that of Eq. (6):

$$\nabla\cdot\left[\frac{k_{SP}k_{\alpha r,SP}}{\mu_{\alpha SP}B_{\alpha SP}}\nabla\Phi_{\alpha SP}\right] + q = \frac{\partial}{\partial t}\left(\frac{\emptyset_{SP}S_{\alpha SP}}{B_{\alpha SP}}\right) \tag{6}$$

where the subscript *SP* denotes that a property from a single-porosity equivalent model. Since $k_{r\alpha}$ itself is a function of S_{α}, and the relations between phase α saturation change rate and $k_{r\alpha}$ depend of the petrophysical behavior of both media, one approach is to define pseudo relative permeability curves that account for relative influence of media in fluid flow.

The first application of pseudo relative permeability in simulation of single-porosity reservoir models is attributed to Hearn (1971). In his work, a stratified reservoir is simulated as a single layer by the usage of pseudo relative permeability curves.

For the simulation of two-phase flow on naturally fractured reservoirs, Klavetter & Peters (1985) proposed the creation of a single-medium equivalent model through the Eqs. (7) to (10):

$$\emptyset_{SP} = \emptyset_f + \emptyset_m \tag{7}$$

$$S_{w,SP} = \frac{S_{wf}\emptyset_f + S_{wm}\emptyset_m}{\emptyset_{SP}} \tag{8}$$

$$k_{SP} = k_f + k_m \tag{9}$$

$$k_{r\alpha,SP}\left(S_{w,SP}\right) = \frac{k_{r\alpha,f}\left(S_{w,f}\right)k_f + k_{r\alpha,m}\left(S_{w,m}\right)k_m}{k_{SP}} \tag{10}$$

where S is the saturation, $k_{r\alpha}$ is the relative permeability to fluid phase α, which can be oil (o) or water (w), and the subscript *SP* refers to a property from the equivalent single-porosity model.

The relative permeability of the equivalent single-porosity model to the phase α at saturation $S_{w,SP}$ is defined as the sum of both fractures and porous matrix relative

permeabilities weighted by their contribution to absolute permeability of the system. The problem with this approach is to determine $S_{w,f}$ and $S_{w,m}$ for a given value of $S_{w,SP}$. The saturations are related with each other by a transfer function, which is dependent of the properties of the rock-fluid system.

Babadagli & Ershaghi (1993) present an experimental work on the subject where relative permeability curves are obtained for different composite systems. The fractured medium is then simulated as a network of fractures and the effect of matrix support is accounted through the effective fracture relative permeability curves. The pseudo curves created by their methodology depend on capillary pressure of matrix, water injection rate and matrix and fracture permeabilities.

Van Lingen et al. (2001) presented a methodology to obtain pseudo relative permeability curves to simulate naturally fractured reservoirs through reservoir properties. Their curves are the same as those defined in Eq. (10) by Klavetter & Peters (1985), but assuming that the fractures are totally filled with water before it reaches into the porous matrix. The method created by them to obtain the curves follows the following steps:

Step 1. Normalize the matrix and fracture relative permeability curves, in order to deal with end points;

Step 2. Determine the parameters α_f, β_{mo} and β_{fw}, which represent the contributions of fractures to total mobile volume, matrix to total oil permeability, and fractures to total water permeability, respectively. Figure 1 presents these parameters, which are determined volumetrically as van Lingen et al. (2001);

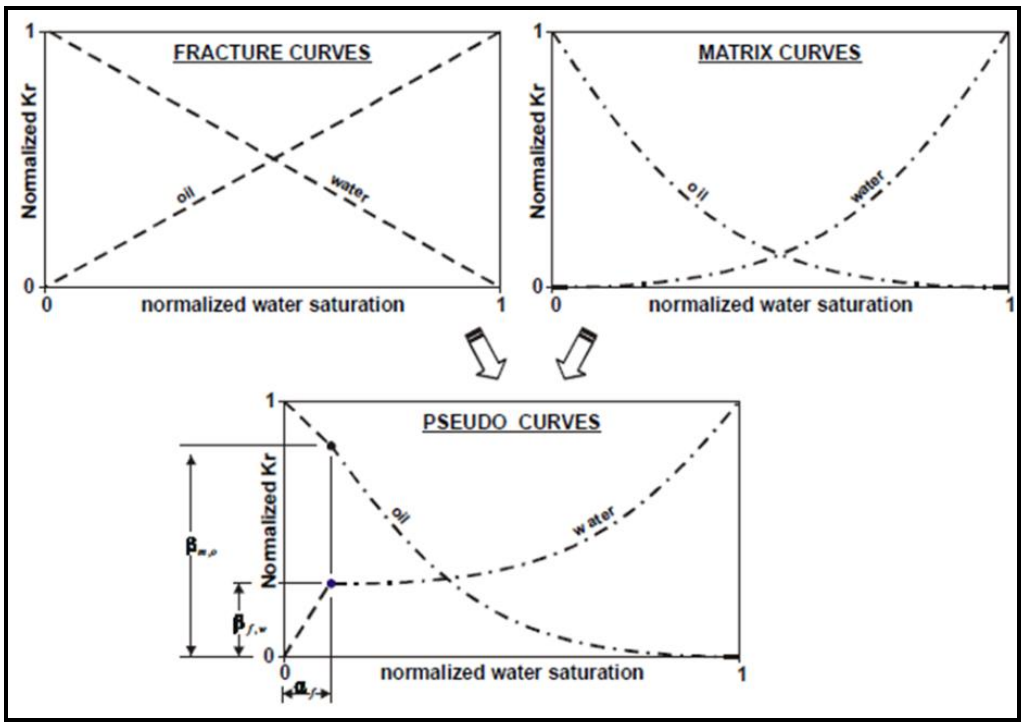

Figure 1: Creation of pseudo relative permeability curves (van Lingen et al., 2001)

Step 3. Construct the normalized pseudo relative permeability curves with the parameters obtained on Step 2. The normalized curves are obtained by Eqs. (11) to (13):

$$S_{wn,SP} = S_{wn,m}\left(1-\alpha_f\right)+\alpha_f \tag{11}$$

$$k_{rwn,SP} = k_{rwn,m}\left(1-\beta_{f,w}\right)+\beta_{f,w} \tag{12}$$

$$k_{ron,SP} = k_{ron,m}\beta_{m,o} \tag{13}$$

where the subscript *n* denotes that the property is normalized.

Step 4. Denormalize the curves based on end points and on residual oil/connate water saturations. To denormalize the curves, it is necessary to have the effective end points for the single porosity model.

If it is assumed that imbibition starts in the porous matrix while the fractures are still filling, then the region before α_f would not rigorously be a straight line. Instead, it would be defined by Eq. 10 as a function of matrix and fracture saturations. But the straight line would still be a possible approximation for the real format. In this sense, the methodology of the present work uses the parameters defined by van Lingen et al. (2001) to represent the behavior of double-porosity models using single porosity equivalent models, following a similar procedure to determine pseudo relative permeability curves. In our case, these parameters are obtained numerically by a calibration process similar to a history matching, in order to create an approximation to two-phase flow behavior of naturally fractured reservoirs.

Abdel-Ghani (2005) presents an improvement for the technique developed by van Lingen et al. (2001) that shows better results for some cases, and worse for others. Gu et al. (2014) present a technique similar to that of van Lingen et al. (2001) and applied it to forecast water flooding performance.

1.2 Defining the model for the simulation of naturally fractured reservoirs

Borbiaux (2010) indicates criteria that may be followed in order to decide which model to use for the simulation of naturally fractured reservoirs. Some of the decision factors pointed are the continuity of the fracture network and the matrix-fracture transfer kinetics.

Accordingly to Bourbiaux (2010), when the fractures create a continuous intercommunicated network the reservoir may be represented as a single medium with pseudo properties, but only when characteristic time for matrix-fracture transfer is significantly shorter than the minimum necessary time step to represent the transport on fractures with some precision. This alternative may not work properly for multiphase flow, since the characteristic time tends to be larger for this case.

2 REFERENCE MODEL MATCHING

First of all, the static properties (porosity and water saturation) of the single porosity equivalent model are obtained in order to match those of the double-porosity model. The values of porosity and initial water saturation of the single-porosity model are defined accordingly to Eqs. (6) and (7), respectively.

The single porosity models are then subjected to a process similar to a calibration process where properties of single porosity models will be iteratively modified until the response produced by them becomes similar enough to the response of the double-porosity model. The automatic optimization method is based on Nelder-Mead simplex with multiple starting points.

The objective function is the Normalized Quadratic Deviance. The function relating the double and single-porosity models is represented as in Eq. (14)

$$NQD = \frac{\sum_{i=1}^{N} \left(DP_i - SP_i\right)^2}{\sum_{i=1}^{N} \left(tol \cdot DP_i\right)^2} \tag{14}$$

where each element of the sum is the comparison between both model responses in each date *i* from the first considered date to the last one, denoted *N*. *DP* and *SP* are the responses from the double-porosity and single-porosity models, respectively, and *tol* is a tolerance index that indicates the maximum tolerated error. This objective function has the advantage of classifying the matching according to the chosen tolerance. The matching is considered successful for values of *NQD* between 0 and 1.

For monophasic flow matching, the objective function takes account the bottom-hole pressure in the production well. The obtained parameter is the absolute permeability. In this case, the models were simulated for 31 days, enough to represent the pressure behavior under monophasic conditions (above bubble pressure).

For the matching of water flood behavior, the objective function is composed by water and oil production and bottom-hole pressure at the producer well, and water injection and bottom-hole pressure at the injector well. The optimized parameters are α_f and β_{mo}. The other parameters needed to create the pseudocurves are defined in terms of β_{mo} as in Eqs. (15) to (17):

$$\beta_{f,w} = \frac{k_{rwe,f}\, k_{roe,m}\left(1-\beta_{m,o}\right)}{k_{rwe,f}\, k_{roe,m}\left(1-\beta_{m,o}\right) + k_{rwe,m} k_{roe,f}\, \beta_{m,o}} \tag{15}$$

$$k_{rwe,SP} = \frac{k_{rwe,f}\, k_{roe,m}\left(1-\beta_{m,o}\right) + k_{rwe,m} k_{roe,f}\, \beta_{m,o}}{k_{roe,m}\left(1-\beta_{m,o}\right) + k_{roe,f}\, \beta_{m,o}} \tag{16}$$

$$k_{roe,SP} = \frac{k_{roe,f}\, k_{roe,m}}{k_{roe,m}\left(1-\beta_{m,o}\right) + k_{roe,f}\, \beta_{m,o}} \tag{17}$$

where the subscript *e* denotes the end-point (largest) value from the property.

Also, is obtained the well productivity index multiplier *mPI*, in order to adjust well bottom-hole pressures. The productivity index is a relation between production rate and pressure drop in a well and in naturally fractured reservoirs it is usually related to the well intercepting or not the fracture planes. If a multiplier *mPI* is applied, it directly changes the value of pressure drop for a given value of production rate. For two-phase reference model matching, the optimization limits values of α_f and β_{mo} between 0 and 1, and values of *mPI* between 0.6 and 3. The models were simulated for 2000 days.

To denormalize the pseudo relative permeability curves, in addition to $k_{rwe,SP}$ and $k_{roe,SP}$, it is necessary to obtain the end point saturations for the composite system ($S_{or,SP}$, and $S_{we,SP}$). These points are obtained according to equations (18) and (19):

$$S_{or,SP} = \frac{S_{or,m}\varnothing_1 + S_{or,f}\varnothing_2}{\varnothing_1 + \varnothing_2} \tag{18}$$

$$S_{we,SP} = 1 - S_{or,SP} \tag{19}$$

where S_{or} and S_{we} are the residual (irreducible) oil saturation and the maximum water saturation, respectively.

During this work, it was considered that flow of water from fractures to matrix occurs only by spontaneous imbibition and, consequently, $S_{or,m}$ is the value of oil saturation in which the capillary pressure in the matrix rock becomes zero. This hypothesis is valid for all evaluated double-porosity models.

The total time for simulation was evaluated for double-porosity models and their respective single-porosity equivalent under waterflooding. To evaluate the influence of simulation grid size on efficiency, a horizontally refined grid was created for each model, both for double-porosity and equivalent single-porosity models.

3 APPLICATION

The studied models represent typical regions between an injector and a producer well in naturally fractured reservoirs. For this study, all tested models are homogeneous and isotropic. The double-porosity models are based on the simulation model presented on Firoozabadi & Thomas (1990). The grid is regular and contains 10x10x10 cells with dimensions of 31.2 m on both horizontal directions and 3.0 m on vertical direction. All simulations were run with black-oil simulator IMEX® from *Computer Modeling Group*®. After the optimization process, we also created a refined grid for each model, composed by 30x30 cells on horizontal and 10 cells on vertical, each with 10.4 m on both horizontal directions and 3.0 m on vertical direction, in order to test the effect of grid size on simulation time.

For matching under monophasic flow conditions, the injector well is closed, while the producer operates with a production rate of 79.5m³/day. For two-phase flow, water is injected at a maximum rate of 159m³/day in order to keep a maximum pressure of 41.4MPa, while the producer well is operating with a max liquid rate of 79.5m³/day. Both wells are completed in all layers.

PVT data, reservoir initial pressure, formation compressibility, and water characteristics are taken from Thomas et al. (1983) and are the same for both double and single-porosity models. The relative permeability curves of the double-porosity are also taken from Thomas et al. (1983) and are presented on Fig. 2 and Fig. 3. The matrix capillary pressure curve is taken from the work of Firoozabadi & Thomas (1990) (Fig. 4), while capillary pressure on the fractures is considered zero. The influence of matrix capillary pressure curve on imbibition is accounted for only through pseudo permeability curves, so capillary pressure on single-porosity models is kept zero.

The properties that vary between different double-porosity models are fracture spacing and matrix and fracture permeabilities and porosities, in order to create models with different values of λ and ω. Variations on k_f were considered independently of λ, since this parameter appears on other terms in dual porosity formulation, so, for each value of k_f tested, models with different values of λ were created by combinations of k_m and L.

In order to have a significant amount of scenarios that could clarify the applicability of the proposed methodology, models were created with 7 values of λ, ranging between $6x10^{-8}$ to $6x10^{-2}$, and 10 different values of ω, ranging from 0.005 to 0.2. Also, aiming to study the effect of $\emptyset_{SP}$ and k_f, these combinations of λ and ω were applied for four combinations of the former parameters, totalizing 280 simulation models.

The value of *tol* in Eq. (14) was set to 0.1, which means that the error tolerance was considered 10% of double-porosity response data (*DP*).

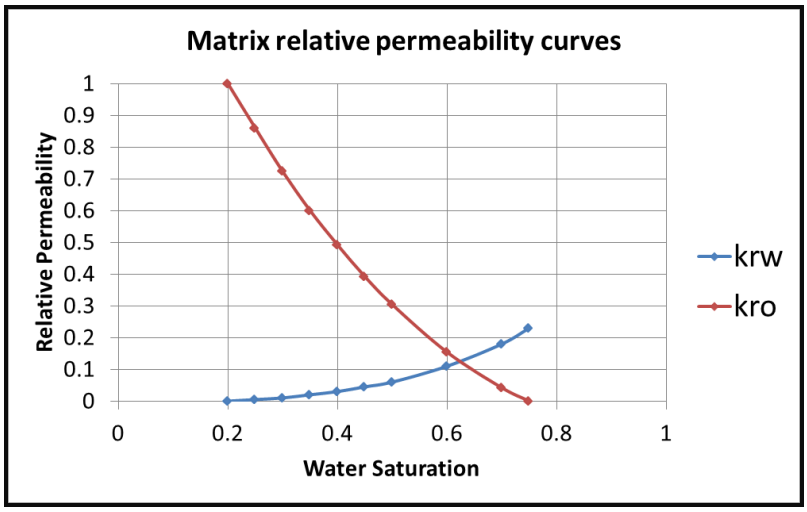

Figure 2: Matrix relative permeability curves for dual-porosity models

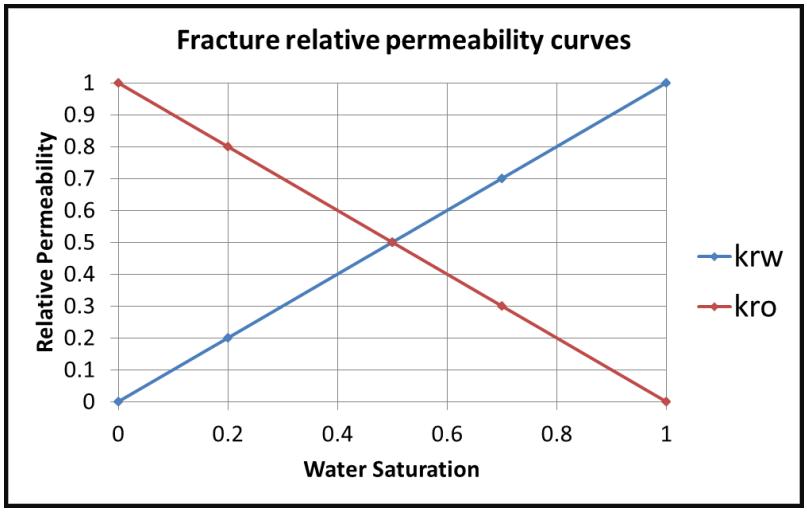

Figure 3: Fracture relative permeability curves for dual-porosity models

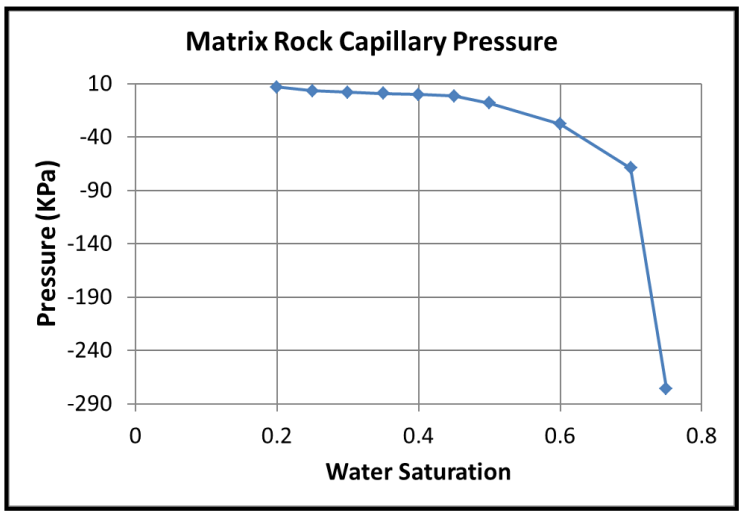

Figure 4: Capillary pressure curve for the matrix domain of dual-porosity models

4 RESULTS AND DISCUSSION

Under monophasic flow conditions, the pressure depletion of all double-porosity models was satisfactorily matched by single-porosity equivalents with a maximum value of *NQD* of $2x10^{-5}$. Figure 5 presents an example of depletion curve matching used to obtain absolute permeability for a single-porosity model.

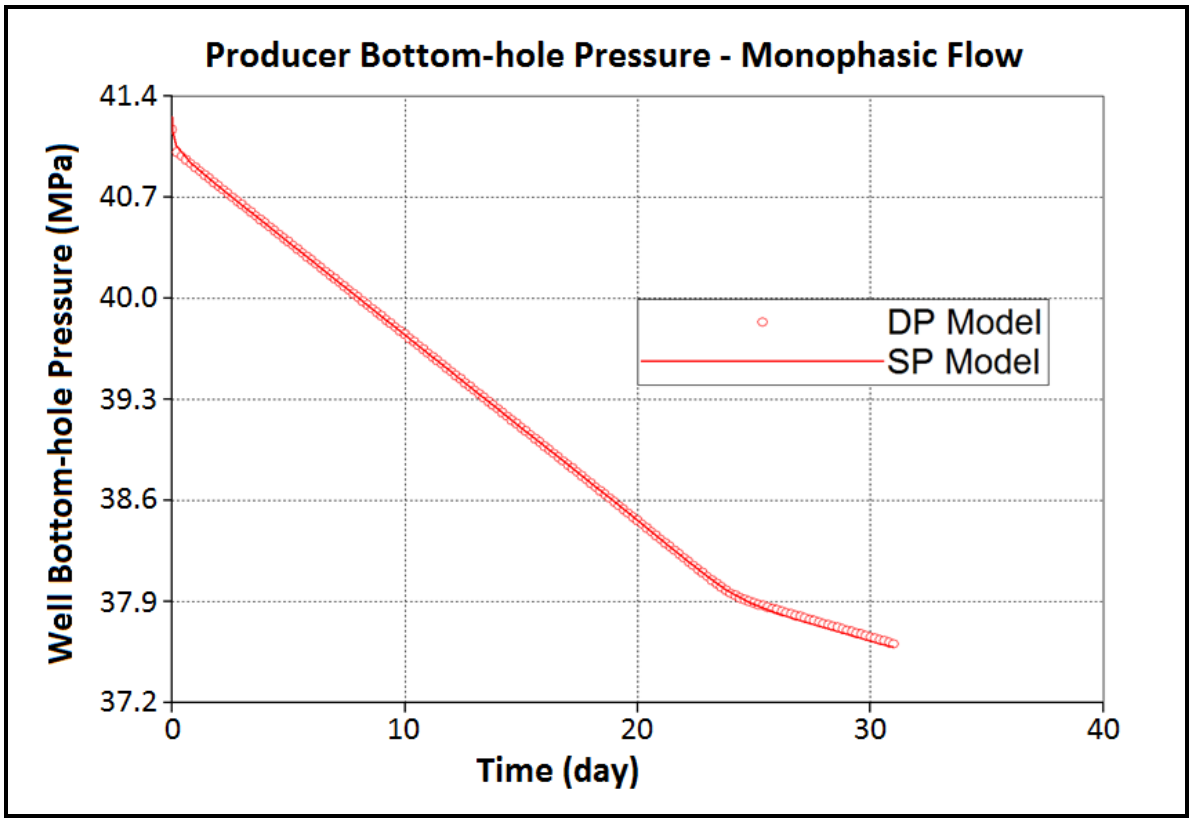

Figure 5: Numerical matching obtained under monophasic flow conditions

For waterflood case, some of the obtained curves are shown in Fig. 6 and Fig. 7**.** For some models, it was not possible to obtain single-porosity equivalents that match double-porosity behavior with *NQD* less than 1. Still, the only objective function that presents *NQD* over 1 for some of the cases is oil rate. The applicability of single-porosity models is conditioned by the parameters λ and ω of the double-porosity model.

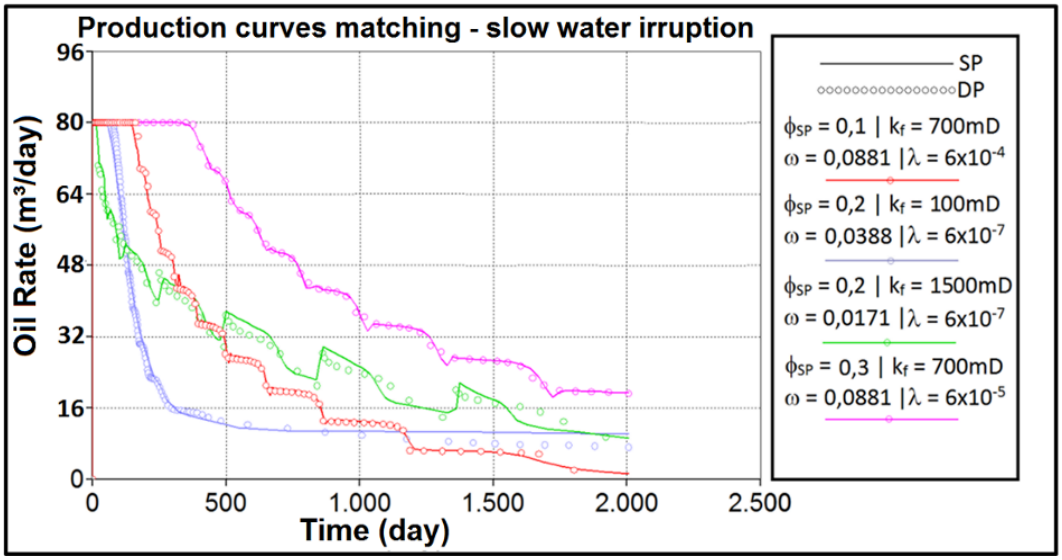

Figure 6: Numerical matching obtained under two-phase flow conditions

Figures 6 and 7 present some examples of matchings between double-porosity (*DP*) and single-porosity (*SP*) models. Figure 6 presents matching curves for models where the water irruption is slow and the behavior is more similar to single-porosity models. For all the matches shown in Fig. 6, the value of *NQD* is close to zero.

Figure 7 presents matches for models where the irruption of the injected water occurs very soon at the producer well. In this case, the behavior is harder to represent through single-porosity equivalent models. The *NQD* for all cases shown is close to 1.

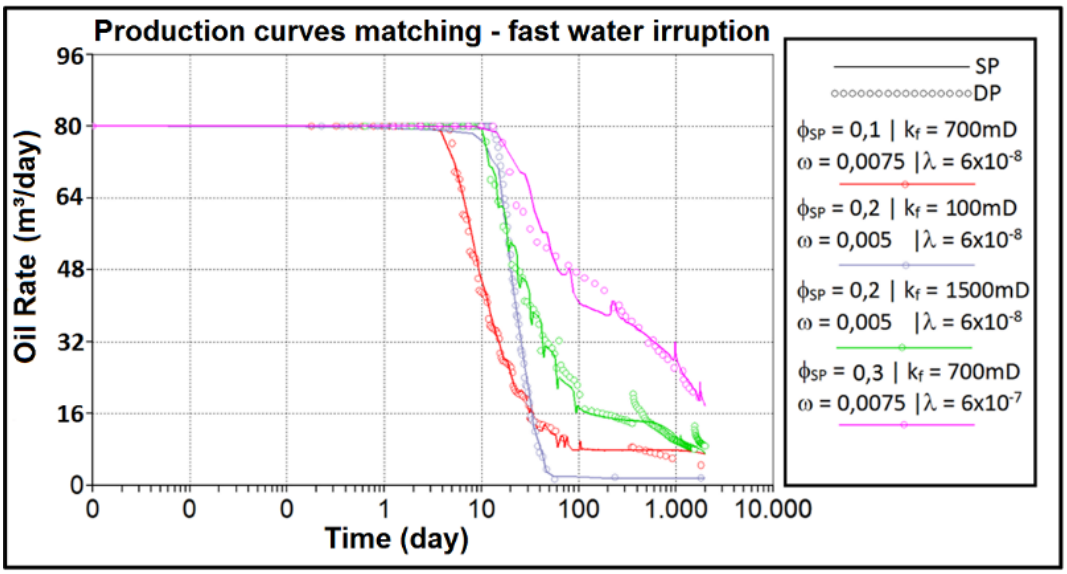

Figure 7: Numerical matching obtained under two-phase flow conditions

Figures 8 and 9 present the quadratic difference of water saturation between single-porosity and double-porosity models distributed along a plane intersecting the injector well. For the model on Fig. 8, the *NQD* for oil rate is approximately 1 (tolerance limit) and for Fig. 9, *NQD* is 0.02. At initial conditions, the models are both adjusted. For advanced times, on models with high *NQD*, the distribution of water is different along entire layers, while for well-adjusted models, high differences on saturation occur only locally in blocks.

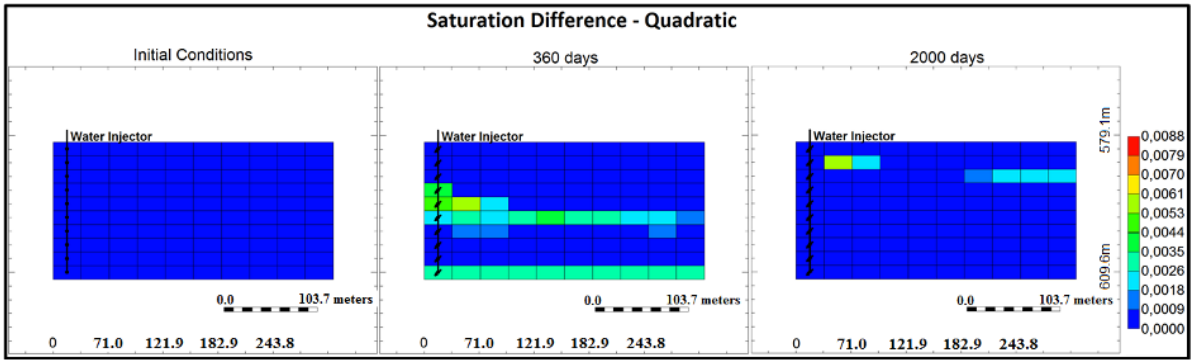

Figure 8: Example of quadratic difference on water saturation between DP and SP models

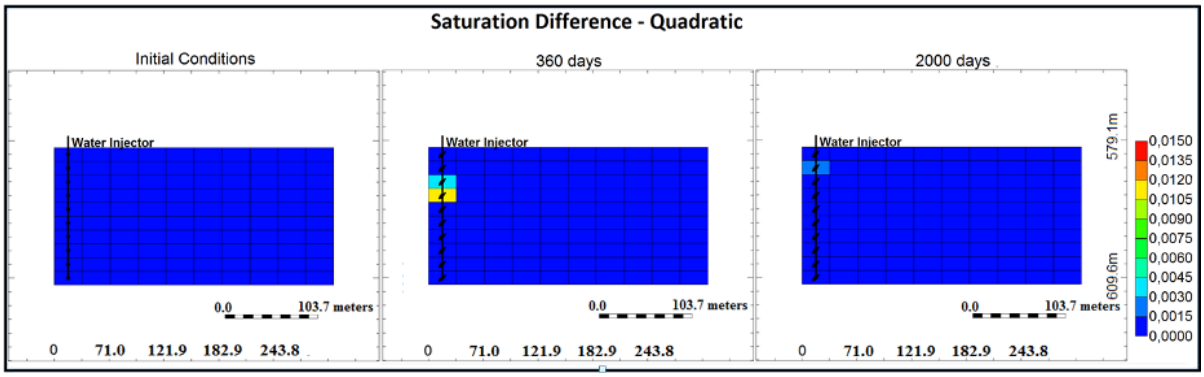

Figure 9: Example of quadratic difference on water saturation between DP and SP models

Figures 10 to 13 show the values of *NQD* obtained for models with different values of λ and ω. Values of *NQD* below 1 were obtained for 271 of the 280 models (97%). The figures show that the double-porosity solution becomes necessary for reservoirs with values of λ below $6x10^{-7}$ and only for ω below 0.085. The errors are larger for larger values of k_f and smaller values of $\emptyset_{SP}$.

The obtained results agree with the conclusions drawn by Borbiaux (2010), which state that if the matrix-fracture transfer is fast enough, the reservoir behaves as a conventional system. Once the system is sufficiently connected, both media react to the pressure gradient simultaneously, avoiding the complexity of the transfer kinetics.

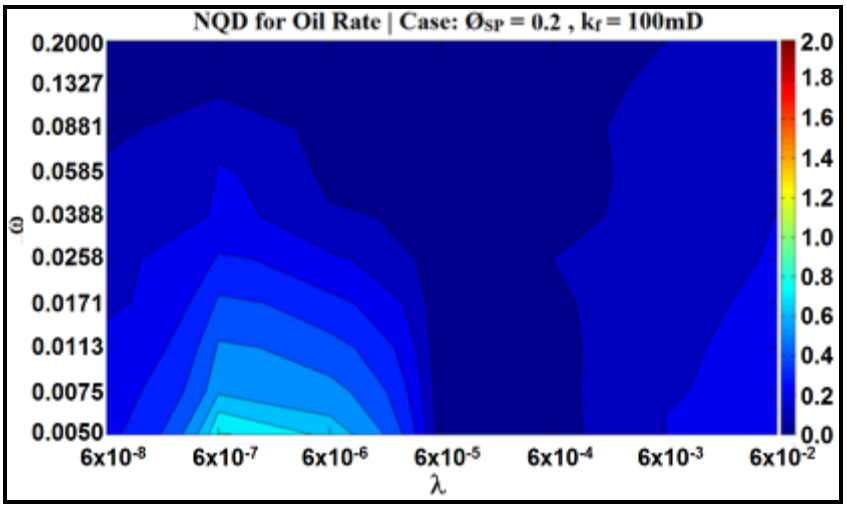

Figure 10: Map of the objective function *NQD* for models with $\emptyset_{SP}$ = 0.2 and k_f = 100mD

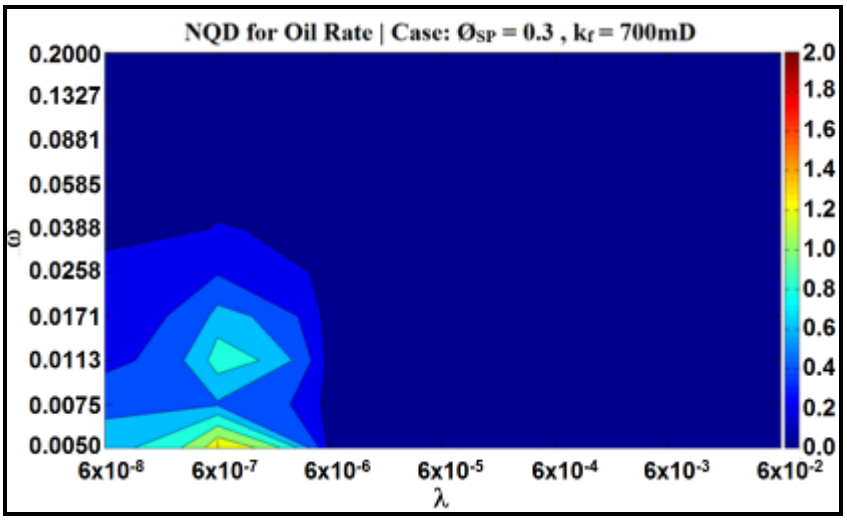

Figure 11: Map of the objective function *NQD* for models with $\emptyset_{SP}$ = 0.3 and k_f = 700mD

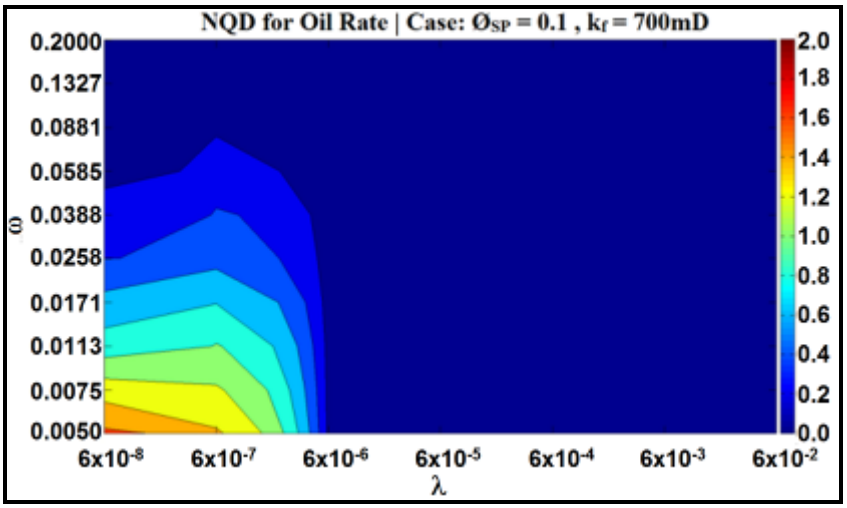

Figure 12: Map of the objective function *NQD* for models with $\emptyset_{SP}$ = 0.1 and k_f = 700mD

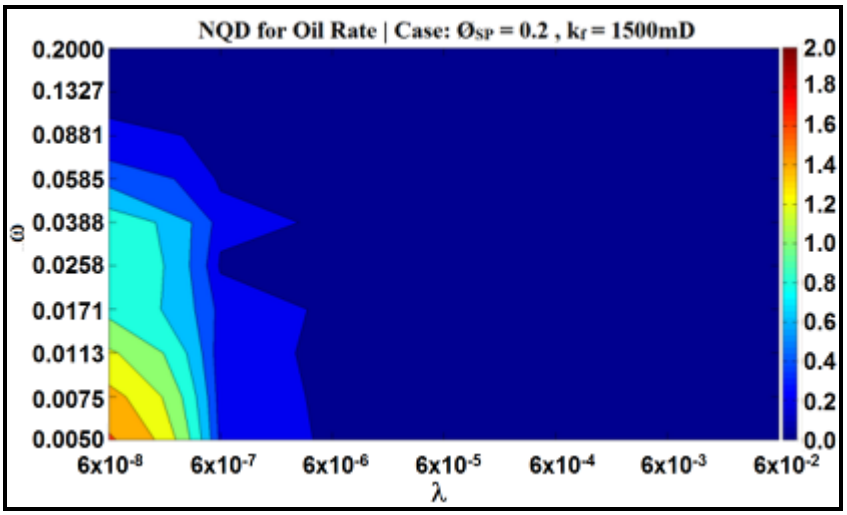

Figure 13: Map of the objective function *NQD* for models with $\emptyset_{SP}$ = 0.2 and k_f = 1500mD

Table 1 presents the values of the ratio between simulation time of the double-porosity and its single-porosity equivalent (t_{DP}/t_{SP}). Each case represents a single value of $\emptyset_{SP}$ and k_f, tested for the 70 combinations of λ and ω. The obtained results show that the benefit from the application of single-porosity models is influenced by the simulation grid block size. For the more refined grid, the ratio between double-porosity and single-porosity simulation times becomes larger, reaching values close to 33.

Table 1 Comparison of computational time for the simulated cases

	$\emptyset_{SP}$ = 0.2 k_f = 100mD	$\emptyset_{SP}$ = 0.1 k_f = 700mD	$\emptyset_{SP}$ = 0.3 k_f = 700mD	$\emptyset_{SP}$ = 0.2 k_f = 1500mD
minimum t_{DP}/t_{SP} (10x10 grid)	0.97	0.20	0.74	0.25
maximum t_{DP}/t_{SP} (10x10 grid)	9.13	17.31	18.02	17.76
mean t_{DP}/t_{SP} (10x10 grid)	2.53	4.47	4.39	5.52
minimum t_{DP}/t_{SP} (30x30 grid)	0.46	0.20	0.41	0.38
maximum t_{DP}/t_{SP} (30x30 grid)	6.58	23.99	21.36	33.49
mean t_{DP}/t_{SP} (30x30 grid)	2.48	5.17	4.91	6.69

Although some single-porosity models present simulation times longer than those of their double-porosity equivalents, this happens only for the case with higher values of fracture permeability and for about 5% of the studied cases. This is related to the parameters used to adjust the pseudo relative permeability curves that may difficult convergence for the model, forcing the simulator to run with small time steps. In addition, this pattern is only observed in the region where the production curves are poorly matched (NQD around 1).

Figure 13 relates the computational time saved by the application of the single-porosity models obtained to the parameters λ and ω. The example shown is for 1500mD of k_f and 20% of $\emptyset_{SP}$, but this pattern is the same in respect to λ and ω for the three studied combinations of k_f and $\emptyset_{SP}$. The methodology is more advantageous for simulating models with higher values of λ. The simulation time for single-porosity models becomes greater for combinations of low values of both λ and ω.

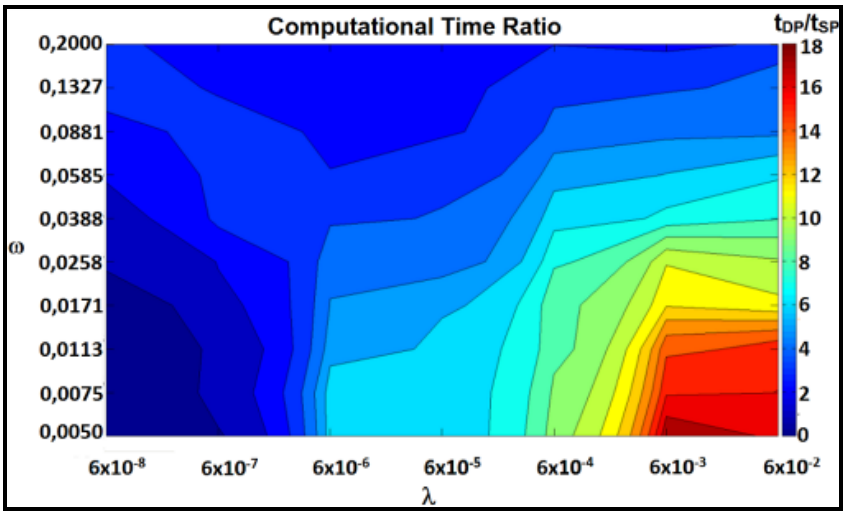

Figure 14: Map of ratio between simulation time for DP and SP models.

5 CONCLUSIONS

According to the presented results, it is possible to obtain equivalent single-porosity models with pseudo properties that simulate monophasic and biphasic water-oil flow in type II naturally fractured reservoirs. For the adjusted cases, the obtained single-porosity models match the production response and water saturation distribution of double-porosity models very closely.

The parameters λ and ω can be used to define the applicability of the technique. For cases in which the matrix-fracture transfer is fast enough (for the range of tested models, all cases when λ is greater than $6x10^{-7}$), the system behaves as a single-porosity system.

The simulation with single-porosity models demands up to 33 times less computational time than double-porosity models. The gain in terms of efficiency can also be defined by the reservoir parameters. The generalization of the methodology may be used as a tool to reduce computational demands for large petroleum reservoir, which may allow for more studies in order to obtain better reservoir management.

Acknowledgements

The authors would like to thank UNISIM, DE-FEM-UNICAMP, CEPETRO, PETROBRAS, FCMG, ANP-FINEP-MCTI through the program PRH-ANP/MCTI and ANP ("Compromisso de Investimentos com Pesquisa e Desenvolvimento") for supporting this work. We also thank CMG for software licenses.

REFERENCES

Abdel-Ghani, R., 2009. Single Porosity Simulation of Fractures With Low to Medium Fracture-to-Matrix Permeability Contrast. In: SPE/EAGE *Reservoir Characterization & Simulation Conference*.

Babadagli, T., Ershaghi, I. 1993. Improved Modeling of Oil/Water Flow in Naturally Fractured Reservoirs Using Effective Fracture Relative Permeabilities. In: *SPE Western Regional Meeting*.

Barenblatt, G. I., Zheltov, Iu. P., Kochina, I. N., 1960. Basic Concepts in the Theory of Seepage of Homogeneous Liquids in Fissured Rocks [Strata]. *Journal of Applied Mathematics and Mechanics*, vol. 24, n. 5, pp. 1286–1303.

Borbiaux, B., 2010. Fractured Reservoir Simulation – a Challenging and Rewarding Issue. *Oil & Gas Science and Technology – Rev. IFP*, vol. 65, n. 2, pp. 227–238

Firoozabadi, A., Thomas, L. K. 1990., Sixth SPE Comparative Solution Project: Dual-Porosity Simulators. *Journal of Petroleum Technology*, vol. 42, n. 6, pp. 710–763.

Gilman, J. R., Wang, H., Fadaei, S., Uland, M. J., 2011. A New Classification Plot for Naturally Fractured Reservoirs. In: *Canadian Unconventional Resources Conference*.

Gu, S., Liu, Y., Chen, Z., Ma, C. 2014. A method for evaluation of water flooding performance in fractured reservoirs. *Journal of Petroleum Science and Engineering*, v. 120, pp. 130–140.

Hearn, C. L., 1971. Simulation of Stratified Waterflooding by Pseudo Relative Permeability Curves. *Journal of Petroleum Technology*, vol. 23, n. 7, pp. 805–813.

Kazemi, H. Merrill Jr., L. S., Porterfield, K. L., Zeman, P. R. 1976. Numerical Simulation of Water-Oil Flow in Naturally Fractured Reservoirs. Society of Petroleum Engineers Journal, vol. 16, n. 6, pp. 317–326.

Klavetter, E.A., Peters, R.R., 1985. Fluid flow in a fractured rock mass. Sandia National Labs., Albuquerque, NM, EUA.

Nelson, R., 2001. Geologic Analysis of Naturally Fractured Reservoirs, second edition. Gulf Publishing Company.

Paiva, H.P., 2012. Simulação da Recuperação de Petróleo em Reservatórios Naturalmente Fraturados. Msc dissertation, Universidade Estadual de Campinas.

Thomas, L. K., Dixon, T. N., Pierson, R. G. 1983. Fractured Reservoir Simulation. *Society of Petroleum Engineers Journal*, v. 23 n. 1, pp. 42–54.

Warren, J. E., Root, P. J., 1963. The Behavior of Naturally Fractured Reservoirs. *SPE Journal of Petroleum Technology*, vol. 3, n. 3, pp. 245–255.

van Lingen, P., Sengui, M., Daniel, J., Cosentino, L., 2001. Single Medium Simulation of Reservoirs with Conductive Faults and Fractures. In: *SPE Middle East Oil Show*.